INFLUENCE OF TRACK MODELLING IN MODAL PARAMETERS OF RAILWAY BRIDGES COMPOSED BY SINGLE-TRACK ADJACENT DECKS

J.C. Sánchez-Quesada*†,E. Moliner†, A. Romero‡, P. Galvín‡ and M.D. Martínez-Rodrigo†

† Department of Mechanical Engineering and Construction
Universitat Jaume I
Castellón, Spain

‡ Escuela Técnica Superior de Ingeniería
Universidad de Sevilla
Sevilla, Spain

e-mail: jquesada@uji.es, molinere@uji.es, aro@us.es, pedrogalvin@us.es, mrodrigo@uji.es

Key words: railway bridges, vertical acceleration, track-bridge interaction, ballasted track, resonance

Abstract: *A significant number of railway bridges composed by simply-supported (SS) spans are present in existing railway lines. Special attention must be paid to short to medium span length structures, as they are prone to experience high vertical acceleration levels at the deck, due to their low weight and damping, compromising the travelling comfort and the structural integrity. The accurate prediction of the dynamic response of these bridges is a complex issue since it is affected by uncertain factors such as structural damping and complex interaction mechanisms such as vehicle-bridge, soil-structure or track-bridge interaction.*

Concerning track-bridge interaction, experimental evidences of a dynamic coupling exerted by the ballasted track between subsequent SS spans and also between structurally independent single-track twin adjacent decks have been reported in the literature. Nevertheless, this phenomenon is frequently disregarded due to the computational cost of models including the track and due to the uncertainties in the mechanical parameters that define the track system.

The present work contributes to the study of the coupling effect exerted by the ballasted track in railway bridges composed by SS adjacent decks. With this purpose a 3D finite element (FE) track-bridge interaction model is implemented with a continuous representation of the track components meshing the sleepers, ballast and sub-ballast with solid FE.

The numerical model is updated with experimental measurements performed on an existing railway bridge in a view to evaluate (i) the influence of the track continuity on the bridge modal parameters and (ii) the adequacy of the implemented numerical model.

1 INTRODUCTION

The ballasted track in railway bridges distributes the axle loads from the rails to the structure, acts as a high-frequency filter and introduces a restraining effect at the end sections [1]. In addition, experimental evidences of load and vibration transfer mechanisms between consecutive spans or adjacent SS decks sharing a continuous ballasted track have been reported over the last years [1, 2]. A vast description of different ballast models developed by researchers in the analysis of train-induced vibrations may be consulted in Reference [3]. These models fall into two main categories: discrete and continuous models. In discrete models the rail displacement is connected to the bridge deck through a set of spring, damper and lumped mass elements generally defined at the sleepers positions that represent the stiffness, damping and mass of the different track components (sleepers, railpads, ballast and sub-ballast), while the

https://doi.org/10.4995/YIC2021.2021.12283

rail is modelled as a continuous beam. From this basis, 2D and 3D representations of the track-bridge interaction have been reported in the scientific literature for different applications [4, 5]. Discrete models are conceptually simple and require less computational effort than continuous models. However they neglect potentially relevant aspects, such as the bending coupling between consecutive SS spans associated to the separation of the ballast and rails from the centre of gravity of the deck cross section and the contribution of the ballast bed to the global deck stiffness.

Continuous track models permit considering the composite action between the track and the bridge associated to the transmission of shear stress between the deck and the rails through the ballast. In these models, the ballast is generally considered as a continuum and is discretised into solid FE [6], admitting elastic and isotropic constant material properties. Additionally, in the ballast regions located at the joints between consecutive spans or decks, a few researchers propose the use of degraded material properties to take into account the possible loss of stiffness of the ballast due to the cyclic movement caused by passing trains [7]. In these works, the degradation is accomplished by reducing the elastic modulus of the general ballast. More refined techniques including the heterogeneous and granular nature of the ballast, such as the Discrete Element Method, are applied for the analysis of settlement and degradation under cyclic loading [8] but they require enormous computational resources which make them unfeasible for application.

The models for ballasted tracks require a significant number of parameters which are highly uncertain. Therefore, a better understanding of their influence is needed in bridge engineering to develop more realistic and adequate numerical tools that, at the same time, do not fall into inadmissible computational costs. In this regard the performance of experimental campaigns on bridges, the development of appropriate calibration methodologies and the experimental-numerical validation becomes crucial. However, the number of reported field measurements performed on multi-span SS viaducts or bridges composed by adjacent decks only coupled through the ballast is scarce to derive general conclusions. Rebelo et al. [1] performed experimental tests on some single-span ballasted railway bridges composed by two adjacent single-track slabs and pointed out the existence of a coupling effect exerted by the shared ballast, which was especially relevant in skewed decks.

In the present work, the authors analyse the coupling effect of the ballasted track taking as starting point Old Guadiana Bridge, a representative railway bridge from a conventional railway line in Spain. The bridge is composed by two identical SS spans and two structurally independent but adjacent single-track decks. A clear dynamic coupling between the spans attributable to the track continuity, and also between the adjacent decks through the shared ballast layer was detected during experimental tests [9]. This work aims to assess the extent of track-bridge interaction effects in such bridges and the key parameters affecting the dynamic coupling between structurally independent parts. With this purpose a 3D FE model is implemented. A degraded type of ballast with elastic anisotropic behaviour is assumed for the regions between subsequent spans or adjacent decks. Finally, the model is updated to reproduce the modal properties identified experimentally.

2 BRIDGE DESCRIPTION

The structure under study is a double-track bridge that belongs to the conventional railway line Madrid-Alcázar de San Juan-Jaén in Spain. It is composed by two identical SS spans of 11.93m length between supports centres. The horizontal structure is formed by two adjacent but structurally independent single-track decks. Each deck is made of a reinforced concrete slab of 0.25 m thickness resting on five pre-stressed concrete girders. The decks are weakly

connected along their longitudinal border through the ballast. Each track is conformed by Iberian gauge UIC60 rails and mono-block concrete sleepers separated 0.60 m [10]. A total ballast thickness "h_b" of 0.45 m is assumed. Underneath the sleepers, the ballast thickness is 0.34 m in accordance with current Spanish regulations [11]. The bridge substructure consists of two external abutments and one central support, and the girders rest on them through laminated rubber bearings.

On May 2019 the response of the bridge was measured to characterise the modal parameters and the dynamic response under operating conditions. Eighteen accelerometers were installed underneath the girders and the vertical response was measured under ambient vibration and several train passages. The accelerometers were installed at points 1 to 18 as indicated in Fig. 1. For details of the experimental campaign the reader is referred to Reference [9].

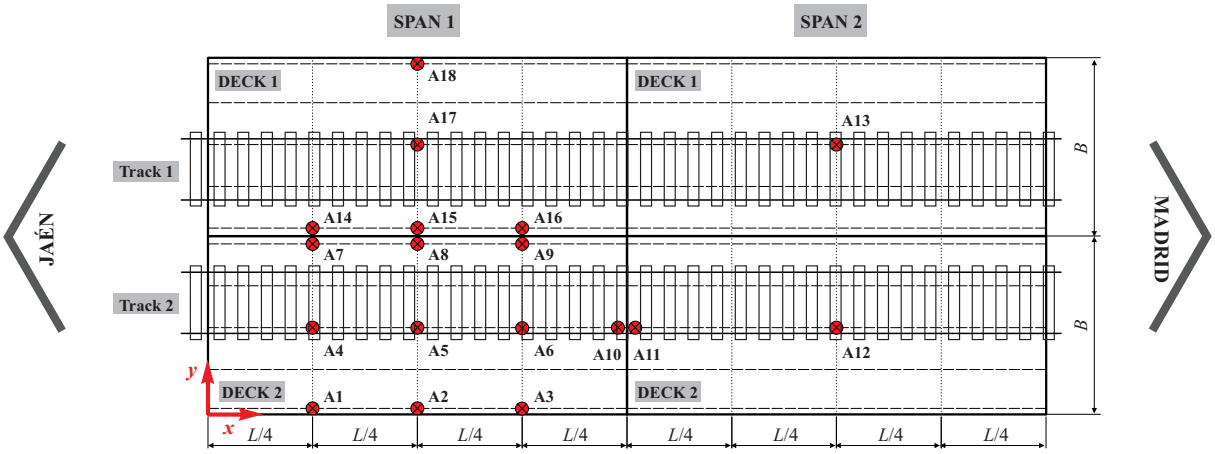

Figure 1: Sensors layout.

Notice that the number of sensors installed was limited, especially in the second span. As a result, the five modes shown in Fig. 3 in red trace (lines and crosses) were identified. The lowest one in frequency order corresponds to the first longitudinal bending mode of each span. The second mode was associated to the combined first torsion mode. In the third mode, the two adjacent decks conform a first transverse bending mode. The fourth and fifth modes were identified as in-phase torsional deformation mode and to the transverse bending mode of each deck, respectively. Fig 3 also provides their natural frequencies (f^{exp}) and modal damping ratios identified from ambient vibration (ξ^{exp}).

3 NUMERICAL MODEL

A 3D continuous track-bridge interaction model of the complete bridge is implemented in ANSYS. The model includes the structure and 15 m of track extension over the embankment before and after the bridge (Fig. 2). The slabs and girders of the bridge are discretised with shell FE, while the laminated rubber bearings with solid FE. The elastic modulus of the bearings was previously calibrated in order to reproduce the experimental static deflection measured during the load test proof of the bridge performed in 2005 [12]. Concerning the track plattform, the sleepers, ballast and subgrade layer are modelled with solid FE. For the rails, Timoshenko beam FE are used, which are connected to the sleepers thorugh the rail pads, considered as discrete spring-dashpot elements. Finally, the handrails are included as lumped masses uniformly distributed along the two external borders of the deck.

An optimisation iterative procedure implemented in ANSYS-MATLAB is performed to minimize an objective function which involves the differences in the predicted and measured natural frequencies and MAC values for the five modes identified from ambient vibration. Based on a

preliminary sensitivity analysis, the optimisation parameters were selected. Successive model samples are generated from variations of these parameters within reasonable limits with respect to nominal values extracted from the project information, scientific literature and current standards. Table 2 shows the main model parameters used in the numerical idealisation of Old Guadiana bridge. Among them, the selected optimisation parameters are those for which variation ranges are provided. In the cited table the following nomenclature is used: E, ν and ρ stand for the elastic modulus, Poisson's ratio, and mass density, respectively. Also, X, Y and Z refer to the longitudinal direction (parallel to the track), transverse and vertical directions, respectively. Concerning the track components, the spring-dashpot discrete properties of the rail pads (K_p and C_p) are provided. The main ballast presents isotropic elastic properties (E_b and ν_b identical in the three directions). The degraded ballast behaviour is considered as transversely isotropic material with elastic constants expressed as E_{bI}, G_{bIJ} and ν_{bIJ}, where I and J refer to the spatial directions X, Y and Z. This material is unequivocally defined by five independent constants:

$$E_{bX} = E_{bY} \qquad E_{bZ} \qquad G_{bXZ} = G_{bYZ} \qquad \nu_{bXY} \qquad \nu_{bXZ} = \nu_{bYZ} \tag{1}$$

In Eq. 1, $E_{bX} = E_{bY}$ are the in-plane elastic moduli, E_{bZ} and $G_{bXZ} = G_{bYZ}$ the out-of-plane elastic and shear moduli, respectively, and ν_{bXY} and $\nu_{bXZ} = \nu_{bYZ}$ the Poisson's ratios.

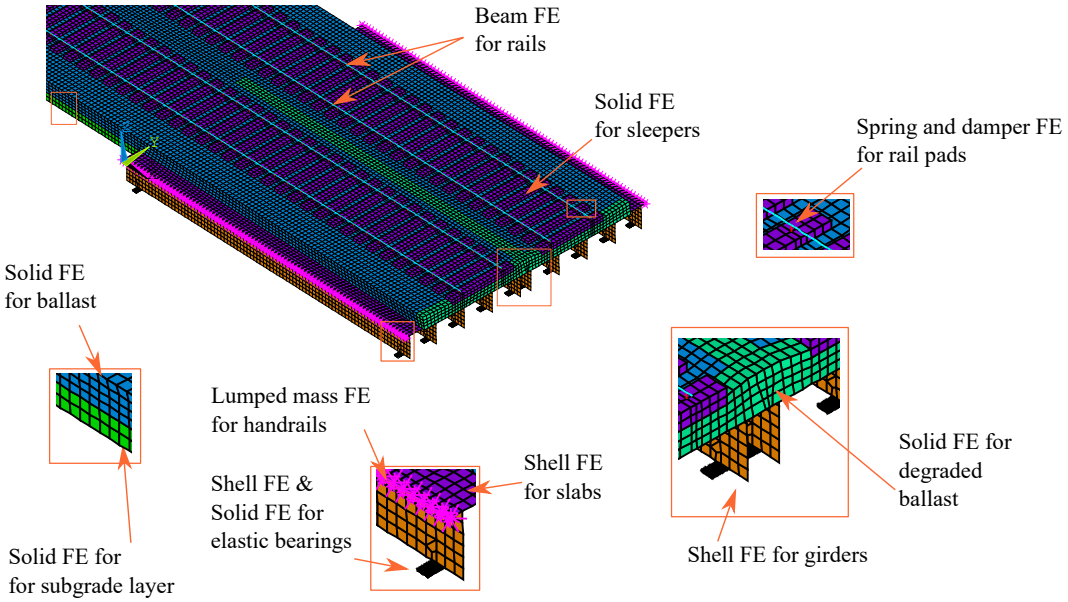

Figure 2: 3D numerical model: detail of one span and track extension.

The experimental and paired numerical mode shapes of the calibrated model are represented in Fig. 3, where the numerical frequency f^{num} is also provided for each paired mode. Table 1 shows the results of the model calibration in terms of frequency differences, calculated as $e_{100\%} = (f^{exp} - f^{num})/f^{exp} \times 100$ and MAC numbers.

Table 1: Frequency differences and MAC numbers of the paired modes after calibration.

Mode (i)	1	2	3	4	5
$e_{100\%}$ [-]	0.47	-3.17	5.37	-2.05	-9.75
MAC [-]	0.94	0.89	0.97	0.93	0.75

As can be seen in Fig. 3, the second and third modes, which are more affected by the continuity of the ballasted track between adjacent decks, are predicted with frequency differences

lower than 5.5%. Also their MAC numbers exhibit a satisfactory correlation with the measurements, with values close to 0.90 or even above. As it is shown, the correspondence of the fifth numerical mode with the experimental measurements is less accurate, even though very reasonable considering the limited number of sensors available in the experimental campaign for the identification of high frequency modes.

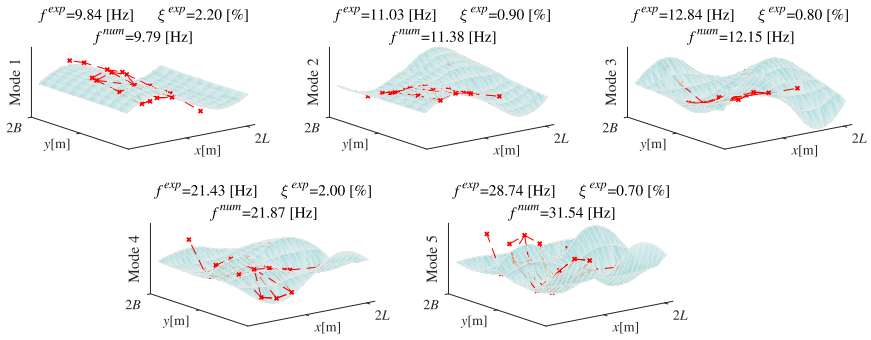

Figure 3: Experimental modes identified (lines path) and calibrated solution (surface)

4 SENSITIVITY ANALYSIS

4.1 Evolution of modal parameters with the thickness of the ballast layer

In this subsection the influence of the thickness of the ballast layer on the modal numerical-experimental correspondence is evaluated. Fig. 4 shows the MAC and $e_{100\%}$ values for the paired numerical modes under variations of the ballast thickness h_b in the range [0.3 – 0.7]m. Experimental frequencies and modal shapes (Fig. 3) are always used as reference values in what follows. The same thickness is assumed for both the main and the degraded ballast regions, based on in situ observations. The rest of the model parameters are kept unmodified and equal to their final updated values. In order to be able to separate the effect of the added mass and the added stiffness that the increase of h_b entails, two different results are provided. First, the total ballast mass is kept invariable, therefore, as h_b increases, the ballast density is modified accordingly and only the extra stiffness affects the results (dashed trace); Secondly, as h_b increases, the ballast density is kept unmodified and equal to its updated final value (and the ballast mass increases proportionally), i.e, both the ballast added mass and stiffness are taken into account (continuous trace). In the plots a black dashed horizontal line indicates a zero difference between the numerical and experimental natural frequencies and a black vertical dash-dot line points out the calibrated value of the elastic property.

From the analysis of the previous figures it can be observed that the fundamental frequency is the one most affected by h_b, leading to a reduction of the numerical frequency as a consequence of the added mass. Its mode shape alteration is negligible as it also is the contribution of the ballast added stiffness. The second (first torsion) mode evolution follows a similar trend, but the numerical frequency reduction is smaller and the effect of the added stiffness is higher when compared to the previous mode. It can also be observed that the natural frequency of the third (transverse bending) mode increases with the thickness of the ballast layer due to the predominant effect of the added stiffness, however its mode shape is only slightly modified. The influence of the ballast thickness on the fourth (second torsion) mode is negligible, but the MAC number reduces remarkably. Finally, the fifth (second transverse bending) mode frequency reduces slightly as the height of the ballast layer increases, and its mode shape remains unaltered.

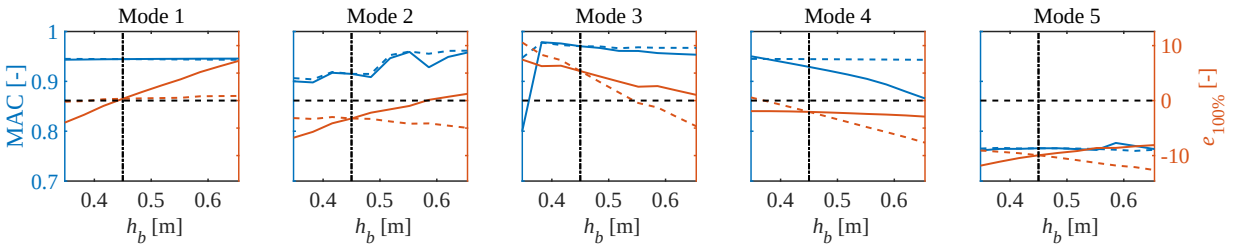

Figure 4: Modal parameters variation in terms of ballast thickness h_b. Dashed trace: constant ballast mass; Continuous trace: constant ballast density.

4.2 Evolution of modal parameters with degraded ballast elastic properties

Finally, a sensitivity analysis is performed in order to analyse the influence of the degraded ballast parameters on the frequency differences and MAC numbers of the paired modes. The parameters that are investigated are the elastic modulus in the vertical direction (Fig. 5), the elastic modulus in longitudinal and transverse directions (Fig. 6) and the independent shear moduli (Fig. 7). These parameters are modified and applied to the degraded ballast along the longitudinal shared border between the adjacent decks and along the transverse shared border between the two spans, separately. In all the cases, the model parameters are kept equal to their final updated value, except for the one that is modified.

In Fig. 5a the MAC and frequency difference $e_{100\%}$ are represented versus E_{bZ} of the degraded ballast along the shared border between the adjacent decks that conform each bridge span, for the five paired modes. In Fig. 5b, the same quantities are represented but the degraded ballast property E_{bZ} is modified only along the transverse border between the spans. Similarly, in Figs. 6a and 6b and in Figs. 7a and 7b the same type of representations are included for the elastic modulus in the horizontal directions $E_{bX} = E_{bY}$ and for the shear modulus in the XZ and YZ planes $G_{bXZ} = G_{bYZ}$, respectively. As in Fig. 4, black dashed horizontal and vertical lines indicate, respectively, zero frequency difference and calibrated value of the model parameter.

From the analysis of the previous figures it can be concluded that the first longitudinal bending mode is the one least affected by the degraded ballast elastic properties. For an acceptable calibration of the frequency of the first torsion mode the elastic modulus in the horizontal directions $E_{bX} = E_{bY}$ must be substantially lower than the vertical elastic modulus E_{bZ} (no higher than 20% of E_{bZ}), both along the longitudinal and the transverse borders. The MAC of the torsion mode is the most affected by the value of the shear modulus in the XZ and YZ planes, $G_{bXZ} = G_{bYZ}$. Both the MAC number and frequency difference for this mode evolve in a similar way for variations of this parameter along both the longitudinal and the transverse borders. The third (first transverse bending) mode is the one most affected by the degraded ballast elastic properties. In this case the frequency difference increases with the reduction of E_{bZ} between the adjacent decks. This effect is also observed for the fourth mode. Nevertheless, the influence of this parameter is not very significant. A minimum value of the elastic modulus in the horizontal directions $E_{bX} = E_{bY}$, both between the adjacent decks and consecutive spans is needed to reproduce the experimental third mode, opposite to what happens with the torsion mode. For values higher than 4×10^7 Pa along the longitudinal border, the model becomes too rigid and the frequency difference is unacceptable. That is not the case for the degraded ballast between the spans. As for the shear modulus $G_{bXZ} = G_{bYZ}$, the value of this parameter does not affect much the MAC of the third mode but the frequency correspondence improves with the increase of this property. As for the fourth (second torsion) mode the influence of the degraded ballast elastic properties between the two spans is almost negligible. In this case the ballast zone affecting the most is $G_{bXZ} = G_{bYZ}$ of the degraded ballast between adjacent decks.

Both, the MAC and frequency difference reduce as this parameter increases. For an accurate prediction of the bridge behaviour a compromise should be found regarding the shear modulus between the second, third and fourth modes, as it affects in opposite ways the modal residuals. Finally, the fifth (second transverse bending) is not affected by either the vertical modulus of elasticity E_{bZ} or the horizontal one $E_{bX} = E_{bY}$ along either of the two edges of the deck. The only parameter affecting this mode is the shear modulus $G_{bXZ} = G_{bYZ}$ of the degraded ballast between spans, which increase leads to a slight improvement in the MAC number.

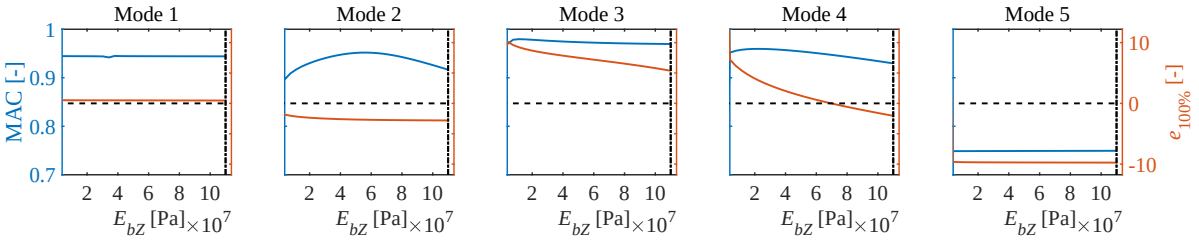

(a) E_{bZ} variations along the longitudinal border between adjacent decks.

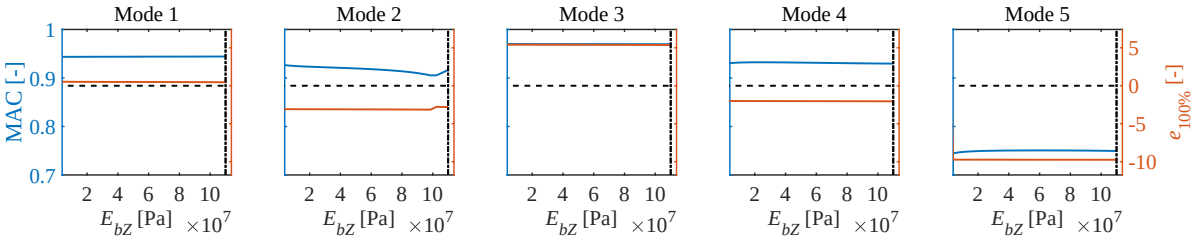

(b) E_{bZ} variations along the transverse border between spans.

Figure 5: Influence of E_{bZ} on the natural frequencies and MAC values.

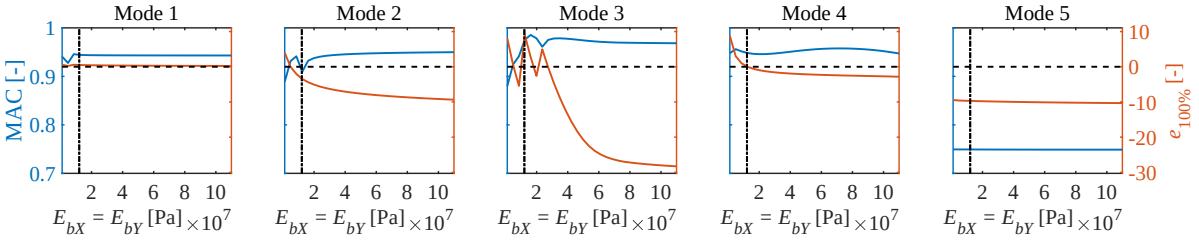

(a) $E_{bX} = E_{bY}$ variations along the longitudinal border between adjacent decks.

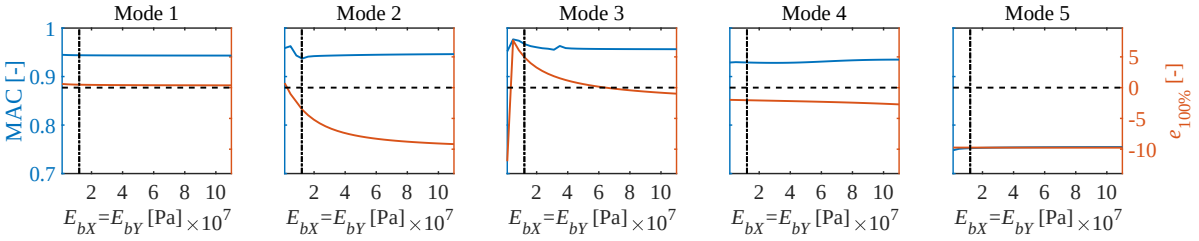

(b) $E_{bX} = E_{bY}$ variations along the transverse border between spans.

Figure 6: Influence of $E_{bX} = E_{bY}$ on the natural frequencies and MAC values.

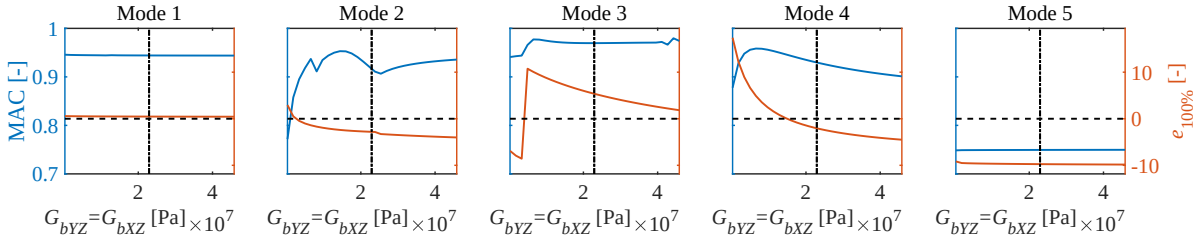

(a) $G_{bXZ} = G_{bYZ}$ along the longitudinal border between adjacent decks.

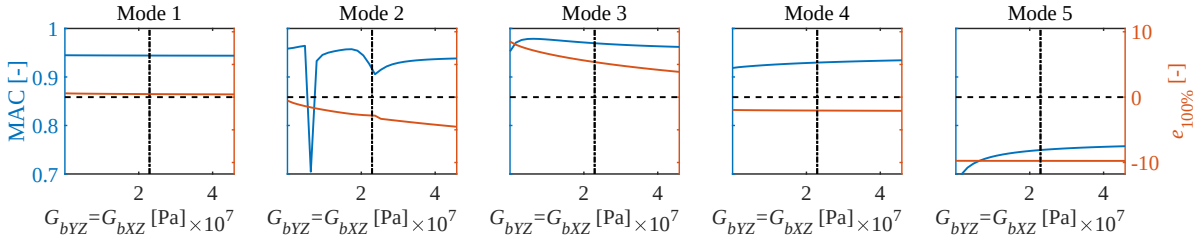

(b) $G_{bXZ} = G_{bYZ}$ variations along the transverse border between spans.

Figure 7: Influence of $G_{bXZ} = G_{bYZ}$ on the natural frequencies and MAC values.

Table 2: Initial and final properties value for track and bridge superstructure.

Bridge component	Notation	Initial value	Calibration range	Calibrated value	Unit
Rail pad	K_p	$1.00 \cdot 10^8$	-	$1.00 \cdot 10^8$	N/m
	C_p	$7.50 \cdot 10^4$	-	$7.50 \cdot 10^4$	Ns/m
Ballast	h_b	0.34	-	0.34	m
	E_b	$1.10 \cdot 10^8$	-	$1.10 \cdot 10^8$	Pa
	ν_b	0.3	-	0.3	-
	ρ_b	1800	$[-30, 30]\%$	1584	kg/m^3
Degraded ballast	E_{bX}=E_{bY}	$1.10 \cdot 10^8$	$[-89, 0]\%$	$12.10 \cdot 10^6$	Pa
	E_{bZ}	$1.10 \cdot 10^8$	-	$1.10 \cdot 10^8$	Pa
	G_{bYZ}=G_{bXZ}	$4.58 \cdot 10^7$	$[-89, 0]\%$	$2.29 \cdot 10^7$	Pa
	ν_{bXY}=ν_{bYX}	0.2	-	0.2	-
	ν_{bXZ}=ν_{bYZ}	0.2	-	0.2	-
	ρ_b	1800	$[-30, 30]\%$	1584	kg/m^3
Handrail	m_b	50	-	50	kg/m
Girders	E_g	$3.60 \cdot 10^{10}$	$[-30, +45]\%$	$4.82 \cdot 10^{10}$	Pa
	ν_g	0.3	-	0.3	-
	ρ_g	2500	$[-30, +30]\%$	2504	kg/m^3
Slabs	E_s	$3.60 \cdot 10^{10}$	$[-30, +35]\%$	$3.10 \cdot 10^{10}$	Pa
	ν_s	0.3	-	0.3	-
	ρ_s	2500	$[-40, +40]\%$	2480	kg/m^3
Elastic bearings	E_{eb}	$2.39 \cdot 10^8$	-	$2.39 \cdot 10^8$	Pa
	ν_{eb}	0.2	-	0.2	-
	ρ_{eb}	1230	-	1230	kg/m^3

5 CONCLUSIONS

In this work the dynamic response of railway bridges composed by SS spans and adjacent single-track decks weakly connected through the ballasted track is investigated. The main aim is to assess the extent of track-bridge interaction effects in such bridges and the key parameters affecting the dynamic coupling between structurally independent parts. With this purpose a 3D FE model is implemented. A degraded type of ballast with elastic anisotropic behaviour is assumed at the regions between subsequent spans or adjacent decks to consider the potential degradation of the ballast due to the relative vertical movements under train passages. The model is updated with experimental results and the main ballast properties affecting the decks coupling are identified and evaluated by means of sensitivity analyses. The following conclusions are derived:

- The updated numerical model is able to reproduce the first five natural frequencies and mode shapes identified experimentally with an average error in the frequencies close to 4% and an average MAC of 0.9, and with a remarkably good correspondence in the particular case of the first longitudinal bending, third transverse bending and fourth second torsion modes.

- In order for the model to reproduce experimental modes higher than the second one, it is essential to consider the coupling effect of the ballast layer, especially between the adjacent decks.

- The predicted natural frequencies and mode shapes are not affected by the degraded ballast elastic modulus between spans in the vertical direction, E_{bz}.

- The first longitudinal bending mode is the one least affected by the degraded ballast elastic properties. In order to obtain a good prediction of the second (first torsion) mode natural frequency the ballast elastic moduli $E_{bX} = E_{bY}$ should be significantly smaller than the vertical elastic modulus E_{bz}.

- The third mode (first transverse bending mode) is the one most affected by the degraded ballast elastic properties. A minimum value of the elastic modulus in the horizontal directions $E_{bX} = E_{bY}$ is needed to reproduce the experimental third mode.

- As per the fourth mode, the most relevant parameter is the shear modulus in the vertical planes $G_{bXZ} = G_{bYZ}$ of the degraded ballast between the decks. Both, the MAC and frequency error reduce as this parameter increases.

- The fifth mode is only affected by the shear modulus $G_{bXZ} = G_{bYZ}$ between the two spans. The MAC number improves as it becomes stiffer.

- Regarding the thickness of the ballast layer, the added stiffness associated to a thicker ballast layer does not affect the fundamental mode. This effect is particularly relevant in the case of the third mode, leading to an important increase in its natural frequency.

6 ACKNOWLEDGEMENTS

The authors would like to acknowledge the financial support provided by the Spanish Ministry of Science and Innovation under research project PID2019-109622RB; FEDER Andalucía 2014-2020 Operational Program for project US-126491; Generalitat Valenciana and Universitat Jaume I under research projects AICO2019/175 and UJI/A2008/06; and the Andalusian Scientific Computing Centre (CICA).

REFERENCES

[1] Rebelo, C. and Simões da Silva, L. and Rigueiro, C. and Pircher, M. Dynamic behaviour of twin single-span ballasted railway viaducts - Field measurements and modal identification. *Engineering Structures*. Vol. **30**, (9), pp. 2460–2469, (2008).

[2] Galvín, P. and Romero, A. and Moliner, E. and De Roeck, G. and Martínez-Rodrigo, M.D. On the dynamic characterisation of railway bridges through experimental testing. *Engineering Structures*. Vol. **226** (111261).

[3] Zhai, W.M. and Han, Z.L. and Chen, Z.W. and Ling, L. and Zhu, S.Y. Train-track-bridge dynamic interaction: a state-of-the-art review. *Vehicle System Dynamics*. Vol. **57**, (7), pp. 984–1027, (2019).

[4] Zhu, Z.H. and Gong, W. and Wang, L.D. and Bai, Y. and Yu, Z.M. and Zhang, L. Efficient assessment of 3D train-track-bridge interaction combining multi-time-step method and moving track technique. *Engineering Structures*. Vol. **183**, pp. 290–302, (2019).

[5] Moliner, E. and Martínez-Rodrigo, M.D. and Galvín, P. and Romero, A. On the vertical coupling effect of ballasted tracks in multi-span simply-supported railway bridges under operating conditions. *International Journal of Mechanical Sciences*.

[6] Malveiro, J. and Ribeiro, D. and Sousa, C. and Calçada, R. Model updating of a dynamic model of a composite steel-concrete railway viaduct based on experimental tests. *Engineering Structures*. Vol. **164**, pp. 40–52, (2018).

[7] Bonifácio, C. and Ribeiro, D. and Calçada, R. and Delgado, R. Dynamic behaviour of a short span filler-beam railway bridge under high-speed traffic. *In: Proc. 2nd Int. Conf. on Railway Technology: Research, Development and Maintenance*, 2014.

[8] Guo, Y. and Zhao, C. and Markine, V. and Jing, G. and Zhai, W.M. Calibration for discrete element modelling of railway ballast: A review. *Transportation Geotechnics*. Vol. **23**, 100341, (2020).

[9] Galvín, P. and Romero, A. and Moliner, E. and De Roeck, G. and Martínez-Rodrigo, M.D. On the dynamic characterisation of railway bridges through experimental testing. *Engineering Structures.*, Vol. **226**, 111261, (2021).

[10] IAPF - Instrucción de acciones a considerar en puentes de ferrocarril, 2010. Ministerio de Fomento, Gobierno de España.

[11] IF3 - Instrucción para el proyecto y construcción de obras ferroviarias, 2015. Ministerio de Fomento, Gobierno de España.

[12] CITEF. *"Informe sobre resultado de registros en puente sobre río Guadiana p.k. 160.000"*. Línea Madrid-Cádiz, tramo Alcázar de San Juan-Manzanares.